The solution structure and heme binding of the presequence of murine 5-aminolevulinate synthase

Brian J. Goodfellow[a], Jorge S. Dias[b], Glória C. Ferreira[c], Peter Henklein[d,1], Victor Wray[e], Anjos L. Macedo[b,*]

[a] *Departamento de Química, Universidade de Aveiro, 3810-193 Aveiro, Portugal*
[b] *Departamento de Química, C.Q.F.B., Faculdade de Ciências e Tecnologia, Universidade Nova de Lisboa, 2825-114 Caparica, Portugal*
[c] *Department of Biochemistry and Molecular Biology, College of Medicine, Institute for Biomolecular Science, and H. Lee Moffitt Cancer Center and Research Institute, University of South Florida, Tampa, FL 33612-4799, USA*
[d] *Institut für Biochemie Peptidsynthese, Charité, D-10098 Berlin, Germany*
[e] *GBF, Mascheroder Weg 1, D-38124 Braunschweig, Germany*

Received 13 July 2001; accepted 8 August 2001

First published online 27 August 2001

Edited by Thomas L. James

Abstract The mitochondrial import of 5-aminolevulinate synthase (ALAS), the first enzyme of the mammalian heme biosynthetic pathway, requires the N-terminal presequence. The 49 amino acid presequence transit peptide (psALAS) for murine erythroid ALAS was chemically synthesized, and circular dichroism and ^{1}H nuclear magnetic resonance (NMR) spectroscopies used to determine structural elements in trifluoroethanol/H_2O solutions and micellar environments. A well defined amphipathic α-helix, spanning L22 to F33, was present in psALAS in 50% trifluoroethanol. Further, a short α-helix, defined by A5–L8, was also apparent in the 26 amino acid N-terminus peptide, when its structure was determined in sodium dodecyl sulfate. Heme inhibition of ALAS mitochondrial import has been reported to be mediated through cysteine residues in presequence heme regulatory motifs (HRMs). A UV/visible and ^{1}H NMR study of hemin and psALAS indicated that a heme–peptide interaction occurs and demonstrates, for the first time, that heme interacts with the HRMs of psALAS. © 2001 Published by Elsevier Science B.V. on behalf of the Federation of European Biochemical Societies.

Key words: Heme binding; 5-Aminolevulinate synthase; Nuclear magnetic resonance structure; Presequence; Target peptide

1. Introduction

In mammalian cells 5-aminolevulinate synthase (ALAS, EC 2.3.1.37) catalyzes the first step of the heme biosynthetic pathway, which occurs in the mitochondrial matrix and involves the condensation of glycine with succinyl-CoA to yield 5-aminolevulinate, carbon dioxide and CoA. At least in non-erythroid cells, this reaction is the rate limiting step in heme production [1–4].

In animals, two separate genes have been identified for ALAS; one encodes the erythroid specific form (ALAS2 or ALAS-E) [5] and the other, the housekeeping gene, encodes the hepatic form of ALAS (ALAS1 or ALAS-H) [6]. Clinically, in the past few years, mutations within the human ALAS2 gene have been identified and established to be the basis of X-linked sideroblastic anemia [7].

ALAS is synthesized in cytosolic ribosomes as a pre-enzyme, which is then imported into and processed within the mitochondria to yield the mature form of the enzyme [8–10]. Human ALAS2 is synthesized as a precursor of molecular mass 65 kDa with an amphipathic presequence (psALAS) of 49 amino acids. During import and processing, the presequence is removed to yield the mature enzyme.

Volland and Urban-Grimal [10] have shown that for yeast ALAS the presequence was not required to target the precursor protein to mitochondria; however, ALAS only reached its final destination, the mitochondrial matrix, when the presequence was present. Thus, in this case, the organelle targeting information appears to reside in the mature protein sequence per se, whereas the subcompartmental (i.e. matrix) information is in the presequence. It was further demonstrated that the targeting information is encoded in non-overlapping regions of the presequence [11].

In general, mitochondrial targeting presequences do not show any sequence homology [12], although functionally, in membrane-like environments, they all form amphipathic α-helices that appear to be important for recognition by the protein import machinery located in the mitochondrial membrane [12,13].

High heme concentration can inhibit the mitochondrial import of ALAS both in vivo and in vitro [8,9,14]. Two heme regulatory elements, containing a single Cys residue (S10-CPVL and R37-CPIL), were identified in the murine ALAS2 presequence as being involved in heme inhibition of the mitochondrial import process [15]. The deletion of heme regulatory motifs (HRM), as well as the mutation of the Cys to Ser residues, was found to reverse heme inhibition.

As a first step in understanding the mechanism of heme inhibition on ALAS mitochondrial import, we have deter-

*Corresponding author. Fax: (351)-21-294 8550.
E-mail address: alm@dq.fct.unl.pt (A.L. Macedo).

[1] Present address: Universitätsklinikum Charitè der Humboldt-Universität Berlin, Institut für Biochemie, D-10117 Berlin, Germany.

Abbreviations: ALAS, 5-aminolevulinate synthase; psALAS, ALAS presequence; NOESY, nuclear Overhauser effect spectroscopy; TOCSY, total correlation spectroscopy; DQF-COSY, double quantum filtered correlated spectroscopy; TFE, trifluoroethanol; SDS, sodium dodecyl sulfate; CD, circular dichroism spectroscopy; TF, target function

0014-5793/01/$20.00
PII: S0014-5793(01)02818-6

mined the global solution structure of murine psALAS, using circular dichroism (CD) and ^{1}H nuclear magnetic resonance (NMR) spectroscopy. The structure was also determined in micellar mimetic environments. In order to identify the presence of heme binding sites in psALAS, UV/visible and NMR titrations were conducted. The results presented here suggest the mechanism by which heme can prevent mitochondrial import of ALAS.

2. Materials and methods

2.1. Peptide synthesis and purification

The ALAS peptide H-Met-Val-Ala-Ala-Ala-Met-Leu-Leu-Arg-Ser-Cys-Pro-Val-Leu-Ser-Gln-Gly-Pro-Thr-Gly-Leu-Leu-Gly-Lys-Val-Ala-Lys-Thr-Tyr-Gln-Phe-Leu-Phe-Ser-Ile-Gly-Arg-Cys-Pro-Ile-Leu-Ala-Thr-Gln-Gly-Pro-Thr-Cys-Ser-NH_2 was synthesized using standard Fmoc methodology on an Applied Biosystems 433A automated synthesizer. TentaGel-R-RAM (Rapp Polymere, Tübingen, Germany) and HBTU coupling reagent (GLS Synthesis Co., Shanghai, PR China) were used. Each synthesis cycle incorporated double coupling of the residues using 10-fold excess of the amino acid. The amino acids Ser, Thr and Tyr were protected by *tert*-butyl, Arg by Pbf and Cys and Gln by the Trt group. The Lys residue was Boc protected. Temporary *N*-α-Fmoc protecting groups were removed by 20% piperidine in *N*-methyl-2-pyrrolidone. The protected ALAS peptide was removed from resin by trifluoroacetic acid (TFA) containing 5% water, 3% triisopropylsilane and 5% 1,2-ethanedithiol.

The crude peptide was purified by preparative HPLC using a VYDAC (40×300 mm) column at a flow rate of 80 ml/min. The solvents used were A = water containing 0.1% TFA and B = 80% acetonitrile (0.1% TFA). The gradient was run between 47 and 97% B over 50 min. The purified peptide yielded a correct ESI mass spectrum (LCQ, Thermoquest).

2.2. Circular dichroism

All CD measurements were made on a Jasco J720 spectropolarimeter at 20°C, using a 0.1 mm path length cylindrical cell with a 1 nm bandwidth, 0.1 nm resolution, 1 s response time and a scan speed of 100 nm/min. Each spectrum was the average of four consecutive scans from 185 to 260 nm, followed by subtraction of the CD signal of peptide-free solutions. The peptide concentrations varied from 30 μM to 150 μM in 2,2,2-trifluoroethanol (TFE)/water solutions (from 20% to 100% (v/v) in TFE) with apparent pH from 2 to 8. TFE was obtained from Sigma (99+%; T6, 300-2).

2.3. UV/visible absorption spectroscopy

Hemin (Porphyrin Products, UT, USA) was solubilized in a 2 M NaOH solution, and a SDS/phosphate buffer solution was added to give final concentrations of 1 mM hemin, 1.5 mM SDS and 10 mM phosphate. The pH was adjusted to 5.4.

Hemin–peptide titrations were followed by UV/visible absorption spectroscopy. Measurements were made on a UNICAM UV2 spectrometer. The spectra were acquired between 300 nm and 750 nm. The hemin solution was dissolved in a 50% TFE/water solution to give a final concentration of 20 μM, which was titrated with the peptide.

2.4. NMR spectroscopy

2.4.1. Sample preparation. The samples for NMR contained 2–3 mg of peptide dissolved in 500 μl of a 1:1 solution of deionized H_2O/TFE-*d2* (Euriso-top, France). The solvents had been previously bubbled with nitrogen to remove any oxygen present. The pH of each solution was adjusted to ca. 3 (uncorrected meter reading) with dilute (0.1 M) HCl. The preparation of the peptide samples in SDS micelles was based on the method of Killian et al. [16]. Equal volumes of a solution consisting of 2–3 mg of the peptide in TFE and a solution of SDS-*d25* were vortexed. The sample was then diluted with deionized water to a final volume of 3 ml and vortexed and lyophilized. The resulting solid was resuspended in 500 μl of H_2O, pH 3, giving a final SDS concentration of 100 mM.

2.4.2. Spectra acquisition. All NMR spectra were recorded on a Bruker DMX600 spectrometer at 300 K. The 2D total correlation spectroscopy (TOCSY) spectra were recorded using a 'clean' TOCSY [17] sequence with a 100 ms mixing time. The 2D nuclear Overhauser effect spectroscopy (NOESY) [18] spectra were recorded with a 150 ms mixing time. The TOCSY and NOESY spectra were recorded with 2048×800 data points, multiplied by a shifted sine-squared window and zero filled to a final size of 2k×2k. The 2D double quantum filtered correlated spectroscopy (DQF-COSY) spectra [19] were recorded with 4096×1024 data points, multiplied by a shifted sine-squared window and zero filled to a final size of 8k×2k.

Spectral processing was carried out using NMRPipe [20], and peak picking, assignment and integration were carried out using SPARKY [21]. The calculation of the solution structures was carried out using DYANA [22] and the manipulation of the structures using MOLMOL [23].

3. Results

3.1. CD experiments

The psALAS peptide was found to be insoluble in 100% water; a mixture of TFE/H_2O was used to dissolve the peptide. CD titrations of a TFE solution of the peptide with water were performed; they showed that the peptide adopts an α-helical conformation (minima at 206 and 222 nm). The minimum TFE percentage for which the peptide presented an α-helix conformation was found to be 50%. Subsequently the behavior of the 50% TFE solution, corresponding to minimum TFE content and maximal helical structure, was monitored with respect to pH (2–5.8) and the peptide concentration (10–150 μM) in order to determine the best experimental conditions for the NMR experiments. The invariance of the CD spectra under all these conditions implied the peptide remained fully dissolved in solution and showed a relatively wide window under which NMR measurements could be performed.

3.2. NMR experiments

A combination of the DQF-COSY and 110 ms TOCSY spectra in 50% H_2O/50% TFE was used to identify the full set of 49 spin systems for psALAS in the TOCSY spectrum. A number of extra, weak spin systems were identified and correspond to systems containing *cis*-proline moieties. The low intensity of these addition signals is compatible with the absence of aromatic moieties adjacent to the proline residues and confirms that the major signals correspond to the all *trans*-proline system [24]. The sequence specific assignment

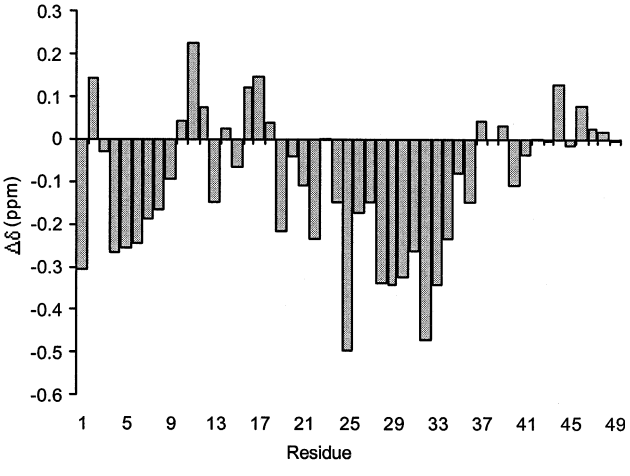

Fig. 1. The chemical shift deviations from random coil values [25] for the Hα resonances of psALAS. An α-helix is indicated, by the sequence of consecutive shift differences greater than −0.1 ppm, for A4–L8 and for L22–S34.

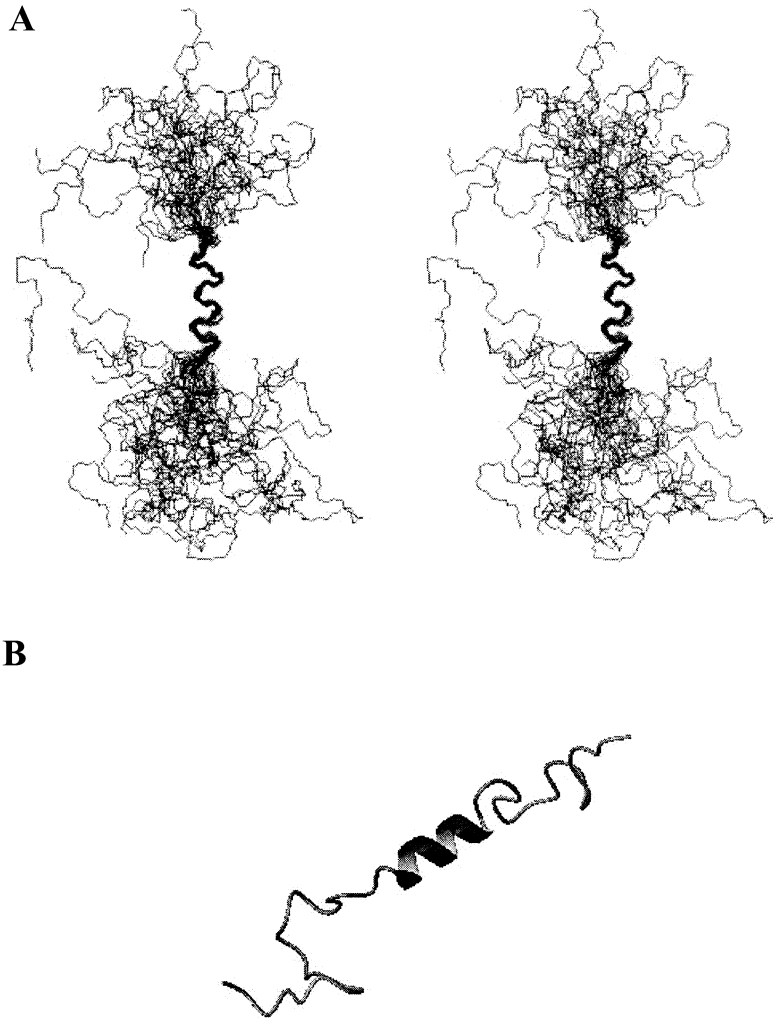

Fig. 2. A: The low TF family of 30 structures of psALAS. The backbone atoms are shown and superposition of the section L22–F33 has been carried out. B: Ribbon diagram showing the secondary structural elements for the structure closest to the mean structure from NMR (calculated by MOLMOL [23]).

of the major spin systems was then determined through inspection of the 150 ms NOESY spectrum.

The identification of secondary structural elements in psALAS was carried out using a qualitative assessment of the NOE pattern and the Hα chemical shift data. Fig. 1 shows the deviation of the Hα chemical shifts from their random coil values for each residue [25]. Using the medium range NOEs, Hα–HN(i,i−3) and Hα–Hβ(i,i+3), observed in the 150 ms NOESY spectrum (supplementary information), an α-helix was identified spanning residues L22 to F33 and is supported by the observation of strong NH-NH(i,i+1) NOEs and the Hα chemical shift data. There are no other obvious regions of structure for the N-terminal region of the peptide from the NOE data, although the Hα chemical shifts data suggests a possible short α-helix for the section A4–R9.

The intensities of the NOESY cross peaks were converted into distance constraints using the CALIBA module of the program DYANA in which a cut-off distance of 6.0 Å was used.

From the integration and calibration of the 386 assigned cross-peaks in the 150 ms NOESY spectrum (corresponding to 58 intra-residue, 77 sequential and 37 medium range

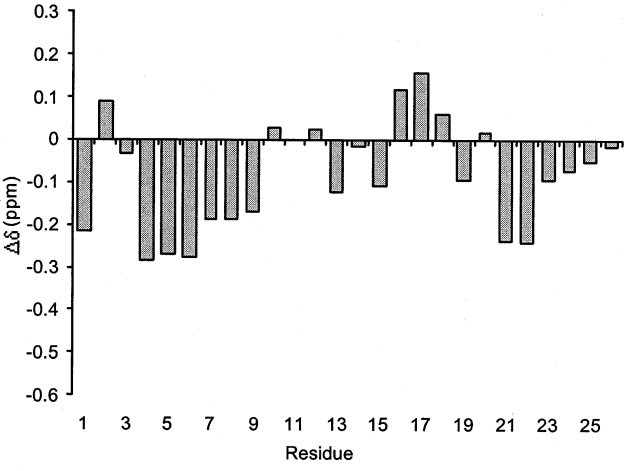

Fig. 3. The chemical shift deviations from random coil values [25] for the Hα resonances of N-psALAS. A short α-helix is indicated by the sequence of six consecutive shift differences greater than −0.1 ppm from A4 to R9.

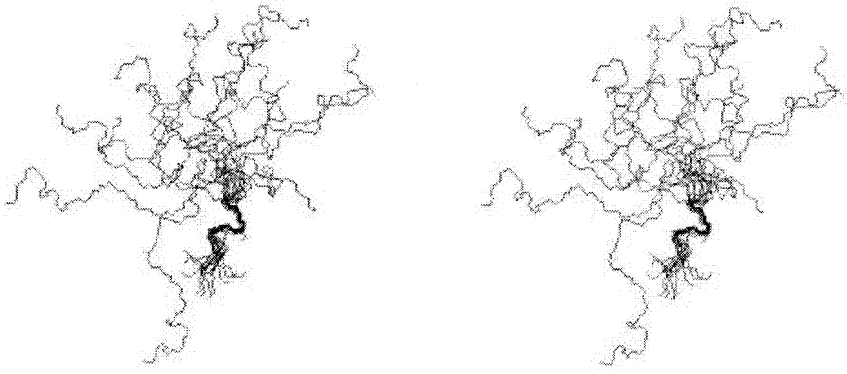

Fig. 4. Stereoview of the low TF family of 15 structures of N-psALAS. The backbone atoms are shown and superposition of the section A4–L8 has been carried out.

NOEs), 172 upper distance limits were obtained. Using these upper limits, 49 lower limits and 20 ϕ/ψ angle constraints from $J_{NH-H\alpha}$ coupling constants, the torsion angle dynamics program DYANA gave a NMR family of 30 structures (protein databank code 1h7d) with target functions (TF) less than 1.15×10^{-2} Å^2 (average TF $5.8\times10^{-2}\pm3.7\times10^{-3}$ Å^2), and with no distance or angle violations. The root mean square deviations (rmsd) between the members of the family and between the mean structure for the backbone atoms for all 49 residues and for residues 22–33 (well defined helix) were 8.30 ± 1.84 Å and 0.67 ± 0.24 Å respectively. A stereoview superposition of these 30 best constrained structures determined from the NMR data after alignment of the G23–F33 α-helix is shown in Fig. 2A, together with a ribbon diagram of the secondary structure elements in the closest structure to the mean NMR structure (calculated by MOLMOL [23]) in Fig. 2B. In order to determine the regions with the lowest rmsd for fitting, consecutive segments (of length one to four residues) of the peptide were compared using a program based on Blankenfeldt et al. [26]. It was found that the region L22–F33 displayed the lowest rmsd (<0.75 Å) coinciding with the well defined α-helix. No other regular structure was readily detectable in any of the final structures. The Hα chemical shift data are in agreement with the observed α-helix. The same data also show six consecutive shift differences greater than −0.1 ppm from A4 to R9 that suggest the presence of a short α-helix, although no medium range NOEs were observed in the NOESY spectrum.

In order to probe the structure of the N-terminus in more detail the 26 amino acid N-terminal fragment of psALAS (N-psALAS) was synthesized and NMR spectra were recorded in 50% TFE. To observe the effect of a more hydrophobic environment on the structure, spectra were also recorded in SDS micelles. The Hα chemical shift data are shown in Fig. 3. In 50% TFE there appears to be very little regular secondary structure from the qualitative NOE data, although again the Hα chemical shift data indicate a short helical region for A4–R9. In SDS, however, the presence of *i,i*+2 and *i,i*+3 NOEs in the region V2–L7 (2–4, 3–5, 5–7 Hα–HN; 4–6, 5–7 HN–HN; 3–6 Hα–HN), and the Hα chemical shift data confirm a stabler structure under these conditions (supplementary information). A family of 15 structures were calculated for N-psALAS in SDS using NOE data from the 150 ms NOESY spectrum (49 intra-residue, 54 sequential and 26 medium range NOEs giving a total of 129 upper distance limits). The torsion angle dynamics program DYANA gave structures with TFs less than 1.6×10^{-2} Å^2 (average TF $1.2\times10^{-2}\pm4.5\times10^{-3}$ Å^2). A fitting based on Blankenfeldt et al. [26] was carried out with the lowest rmsd (<0.75 Å) coinciding with the region

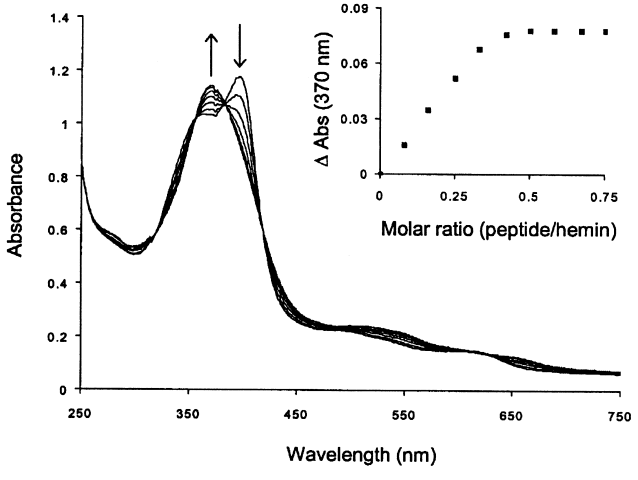

Fig. 5. Absorption spectra of hemin/psALAS titration, showing the characteristic hemin Soret band at 388 nm, decreasing in intensity on psALAS addition. A new band at 371 nm appears due to the hemin/psALAS interaction. The inset shows the variation of the intensity at 370 nm as a function of the hemin/psALAS molar ratio, indicating that an interaction is taking place with a stoichiometry of approximately 2:1. This stoichiometry is consistent with two hemin molecules interacting with the two HRMs present in one psALAS molecule.

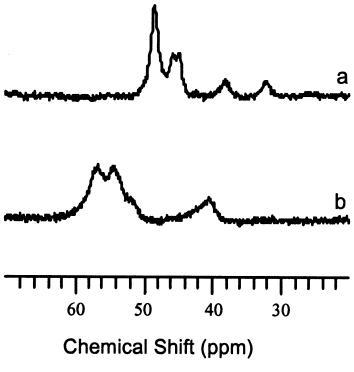

Fig. 6. Low field region of 1D ^{1}H NMR spectra of (a) hemin solution, pH 5 and (b) psALAS 50% TFE, pH 5 after addition of 25% equivalent of hemin.

A4–L8. An analysis of the structures in the family (protein databank code 1h7j) showed that this region is mainly α-helical (Fig. 4). Although only four of the 15 have 'classic' α-helical structure, the Ramachandran plot of the NMR family indicates that the residues A4–L8 all fall within core or allowed α-helix regions of the plot.

3.3. Heme interactions

The presence of heme is known to inhibit the import of ALAS into mitochondria [8,14,15]. Therefore, in order to address, at a structural level, the mechanism of inhibition, UV/visible titrations were initially used to study the psALAS/heme interaction. Using the characteristic heme absorption spectrum [27], a hemin solution was titrated with the psALAS peptide. The Soret band, with a maximum at 388 nm, shifted to a shorter wavelength of 370 nm on addition of psALAS (Fig. 5), indicating that an interaction is taking place. The change in absorbance at 370 nm plotted as a function of the molar ratio (psALAS/hemin) shows a 1:2 relationship (Fig. 5, inset). This stoichiometry is consistent with two hemin molecules interacting with the two HRMs present in one psALAS molecule. A titration of hemin with N-psALAS presented similar shifts in the Soret band (to 370 nm), although here the stoichiometry was 1:1, due to the presence of only one of the HRMs in the smaller N-psALAS peptide.

The hemin/psALAS interaction was also probed by ^{1}H NMR spectroscopy. The presence of a high spin Fe^{3+} atom ($S = 5/2$) induces paramagnetic shifts in the protons of the porphyrin ring, due to transfer of spin density from the Fe atom. A comparison between a hemin solution and a psALAS–hemin mixture indicated that there were clear differences in the low field region of the 1D proton spectra for these resonances (Fig. 6). If heme–psALAS interactions are present, shifts for the hyperfine shifted hemin resonances would be expected, due to a change in the distribution of the electron spin density resulting from the interaction. Also, the fact that the resonances are broader than those for the free hemin may indicate equilibrium between the free hemin and the hemin/peptide complex. The observed low field shift of the porphyrin resonances in the presence of psALAS is also consistent with a change in coordination number for the Fe. A NMR study of Fe(III) protoporphyrin IX [28] showed the methyl resonances appearing downfield at 50–55 ppm when no axial ligands are present. When the Fe was 5- or 6-coordinate the methyl resonances shifted to 55–65 ppm. Thus the shifts observed on the introduction of psALAS to hemin are consistent with axial coordination of the Fe atom. Electron paramagnetic resonance spectra were also obtained for the hemin and hemin/peptide samples (data not shown), presenting characteristic $g \approx 6$ features indicative of the presence of a high spin Fe^{3+} [29]. The differences in g features seen by peptide addition can be attributed to a change in axial coordination, namely, a water molecule that has been replaced by an interacting ligand which maintains the weak ligand field. Interaction of the sulfur atom of a cysteine residue would maintain this weak field.

4. Discussion

The widely accepted import process by which ALAS (or any mitochondrial protein) is transported into the mitochondria includes many steps [12], one of the most important being the initial recognition step involving the N-terminal presequence. Translocase of the outer membrane (TOM) and translocase of the inner membrane (TIM) protein complexes appear responsible for recognition and import through the mitochondrial membrane [12]. The protein Tom20 is anchored to the mitochondrial outer membrane, and its interaction with presequences is thought to be the recognition step which allows subsequent import. A number of studies have shown that an amphipathic N-terminal α-helix is a requirement for mitochondrial presequences and that positive charges, present at the N-terminal in almost all known presequences, are also essential [12]. A recent NMR study of a complex between rat Tom20 and a 10 amino acid presequence from the C-terminus of the aldehyde dehydrogenase presequence [30] showed that a hydrophobic patch on the Tom20 protein is used to recognize presequences, the hydrophobic region of the presequence interacting with this patch and the hydrophilic region interacting with solvent or negatively charged side chains from Tom20. Mutation studies suggested that presequence interaction with Tom20 occurs via hydrophobic interactions and that the presence of positive charges in the presequence is non-essential for recognition [30]. The positive charges are, therefore, thought to be required further along the recognition import chain.

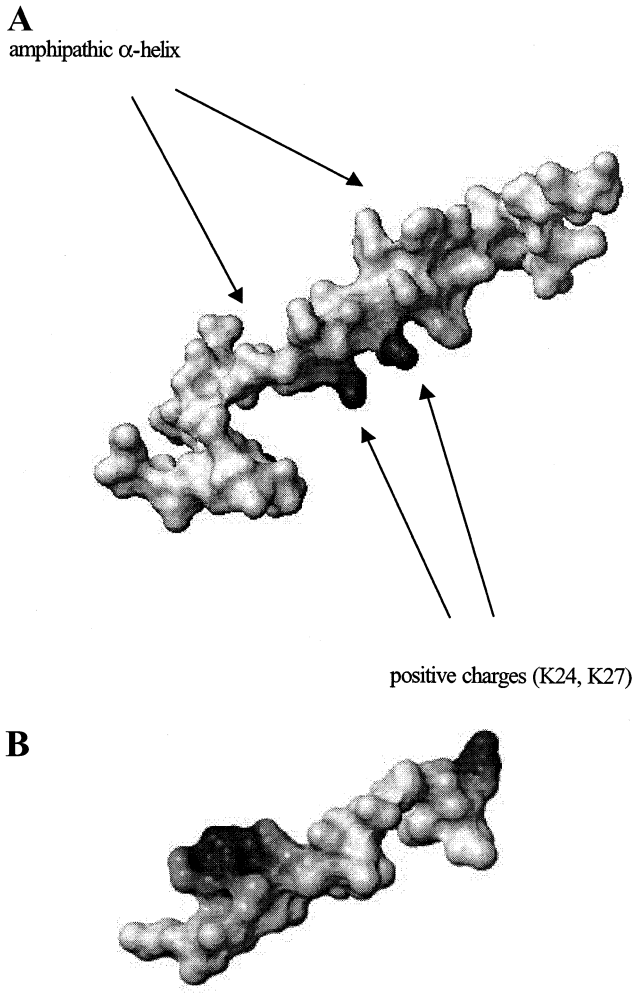

Fig. 7. Surface representation showing the charge distribution (black = positive) for the amphipathic α-helix at (A) L22–F33 and (B) A4–R9 for the closest structure to the mean NMR structure for psALAS and N-psALAS respectively.

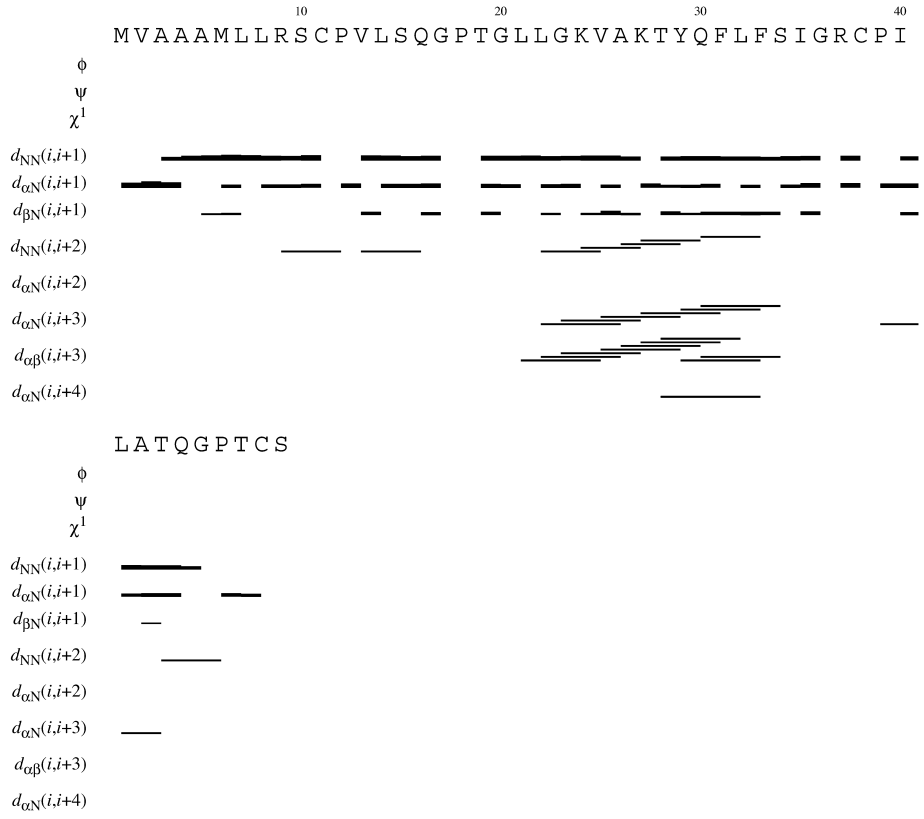

Fig. A1. Summary of sequential and medium range NOE connectivities observed for psALAS in 50% TFE. The intensities of sequential NOEs are categorized as strong, medium and weak and are represented by the thickness of the lines.

A recent study of the interaction of the presequence peptide of mitochondrial aspartate aminotransferase with model membranes [31] suggested that the N-terminal portion of the 29 amino acid presequence mediates binding to the membrane. It was also suggested, using secondary structure prediction methods, that a second amphipathic helical segment is present and that this helix may be the Tom20 recognition element for mitochondrial import.

Our present study has shown that, in 50% TFE, the 49 amino acid psALAS exists as an amphipathic helix, at L22–F33, with a positively charged surface provided by two lysine residues (Fig. 7A) and no stable helix at the N-terminus. The results for the shorter 26 amino acid N-terminal N-psALAS (which contains eight hydrophobic residues, followed by an arginine) also indicate a lack of stable structure in 50% TFE. However, in the more hydrophobic environment of micelles a short helix is formed. Fig. 7B shows an electrostatic surface for the mean NMR structure of N-psALAS in SDS, where it can be seen that the short helix is amphipathic, the hydrophobic side involving three alanines and two leucines and the hydrophilic side a positive arginine residue. It appears, therefore, that psALAS has the characteristics common to all mitochondrial presequences: positively charged residues, a propensity to form an amphipathic N-terminal α-helix in membrane-like hydrophobic environments, and a second helical structural element.

High heme concentrations inhibit the translocation of the ALAS precursor into mitochondria [8,14,15]; thus conceivably, heme could control not only the ALAS mitochondrial import but also the heme biosynthetic pathway. The results from the present heme–peptide interaction studies demonstrate that heme interacts at a 2:1 ratio with psALAS and at a 1:1 ratio with N-psALAS and the ligand that interacts does so maintaining a weak ligand field at the Fe. These results combined with the recognition that there are two HRMs in psALAS and that both contain Cys (S when bound to Fe will maintain a weak field) suggest that heme is interacting with the Cys in the HRM. The shifts seen in the UV/visible titrations are also very similar to those seen (388–362 nm) for titrations of hemin with a peptide containing the HRM of HAP1 where cysteine binding also occurs [27].

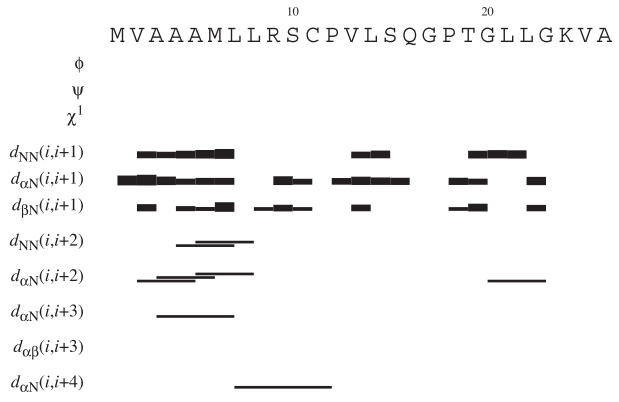

Fig. A2. Summary of sequential and medium range NOE connectivities observed for N-psALAS in 50% TFE and SDS. The intensities of sequential NOEs are categorized as strong, medium and weak and are represented by the thickness of the lines.

Structurally, the first HRM is very close to the N-terminal helix, with the side chain of C11 directed toward the hydrophobic side of this helix. If heme interacts at this site, the initial recognition between the membrane and the N-terminal helix would be affected due to changes in the charge/hydrophobicity induced by the presence of heme and hence anchorage of the presequence in the membrane would be more difficult. The same argument can be applied to the second HRM which follows the well defined helix at L22–F33. In this case interference with the interaction of this region with the hydrophobic patch on the import receptor of Tom20 would be more difficult. Thus in this model the heme interaction prevents or severely modifies those areas of the peptide with a propensity for helical formation coming into contact both with the membrane and with the hydrophobic regions of the receptor(s), most probably through disruption of the hydrophobic environment necessary for helix formation of the presequence. Hence our results are consistent with an interaction model involving two recognition elements: the short N-terminal hydrophobic region, which becomes structured in the presence of membrane mimetic environments, and a longer well defined α-helix which can interact with a hydrophobic patch on Tom20 or another import receptor.

Acknowledgements: We would like to thank João Pessoa and Isabel Correia, I.S.T., Lisbon, for their help in CD measurements. This work was supported by Fundação para a Ciência e Tecnologia, Grant PRAXIS/C/BIA/10086/1998 (A.L.M.) and the National Institutes of Health (Grant DK52053 to G.C.F.).

Supplementary information

(*see page before*) Fig. A1 - A2

References

[1] Ferreira, G.C. and Gong, J. (1995) J. Bioenerg. Biomembr. 27, 151–159.
[2] Kappas, A., Sassa, S., Galbraith, R.A. and Nordmann, Y. (1995) in: The Metabolic and Molecular Basis of Inherited Disease (Scriver, C.R., Beaudet, A.L., Sly, W.S. and Valle, D., Eds.), pp. 2103-0000, McGraw-Hill, New York.
[3] Ponka, P. (1991) Blood 89, 1–25.
[4] Ferreira, G.C. (1999) in: Inorganic Biochemistry and Regulatory Mechanisms of Iron Metabolism (Ferreira, G.C., Moura, J.J.G. and Franco, R., Eds.), pp. 15–34, Wiley-VCH, Weinheim.
[5] Cotter, P.D., Willard, H.F., Gorski, J.L. and Bishop, D.F. (1992) Genomics 13, 211–213.
[6] Bishop, D.F., Henderson, A.S. and Astrin, K.H. (1990) Genomics 7, 207–214.
[7] Bottomley, S.S. (1999) in: Wintrobe's Clinical Hematology (Lee, G.R., Ed.), pp. 1022–1045, William and Wilkins, Baltimore, MD.
[8] Yamauchi, K., Hayashi, N. and Kikuchi, G. (1980) J. Biol. Chem. 255, 1746–1751.
[9] Srivastava, G., Borthwick, I.A., Brooker, J.D., Wallace, J.C., May, B.K. and Elliott, W.H. (1983) Biochem. Biophys. Res. Commun. 117, 344–349.
[10] Volland, C. and Urban-Grimal, D. (1988) J. Biol. Chem. 263, 8294–8299.
[11] Haldi, M. and Guarente, L. (1989) J. Biol. Chem. 264, 17107–17112.
[12] Neupert, W. (1997) Annu. Rev. Biochem. 66, 863–917.
[13] Killian, J.A. and von Heijne, G. (2000) Trends Biochem. Sci. 25, 429–434.
[14] Hayashi, N., Watanabe, N. and Kikuchi, G. (1983) Biochem. Biophys. Res. Commun. 115, 700–706.
[15] Lathrop, J.T. and Timko, M.P. (1993) Science 259, 522–525.
[16] Killian, J.A., Trouard, T.P., Greathouse, D.V., Chupin, V. and Lindblom, G. (1994) FEBS Lett. 348, 161–165.
[17] Greisinger, C., Otting, G., Wüthrich, K. and Ernst, R.R. (1988) J. Am. Chem. Soc. 110, 7870–7875.
[18] Macura, S. and Ernst, R.R. (1980) Mol. Phys. 41, 95–117.
[19] Piatini, U., Sorensen, O.W. and Ernst, R.R. (1982) J. Am. Chem. Soc. 104, 6800–6801.
[20] Delaglio, F., Grzesiek, S., Vuister, G., Zhu, G., Pfeifer, J. and Bax, A. (1995) J. Biomol. NMR 6, 277–293.
[21] Goddard, T.D. and Kneller, D.G. (2000) http://www.cgl.ucsf.edu/home/sparky/.
[22] Güntert, P., Mumenthaler, C. and Wüthrich, K. (1997) J. Mol. Biol 273, 283–298.
[23] Koradi, R., Billeter, M. and Wüthrich, K. (1996) J. Mol. Graphics 14, 51–55.
[24] Grathwohl, C. and Wüthrich, K. (1976) Biopolymers 15, 2025–2041, 2623–2633.
[25] Merutka, G., Dyson, J.H. and Wright, P.E. (1995) J. Biol. NMR 5, 14–24.
[26] Blankenfeldt, W., Nokihara, K., Naruse, S., Lessel, U., Schomburg, D. and Wray, V. (1996) Biochemistry 35, 5955–5962.
[27] Zhang, L. and Guarente, L. (1995) EMBO J. 14, 313–320.
[28] Budd, D.L., La Mar, G.N., Langry, K.C., Smith, K.M. and Nayyir-Mazhir, R. (1979) J. Am. Chem. Soc. 101, 6091–6096.
[29] Moore, G.R. and Pettigrew, G.W. (1990) in: Cytochromes c. Evolutionary, Structural and Physicochemical Aspects, pp. 27–107, Springer-Verlag, Berlin.
[30] Abe, Y., Shodai, T., Muto, T., Mihara, K., Torii, H., Nishikawa, S.-I., Endo, T. and Kohda, D. (2000) Cell 100, 551–560.
[31] Doñate, F., Yañez, A.J., Iriate, A. and Martinez-Carrion, M. (2000) J. Biol. Chem. 275, 34147–34156.